


## Stem-Cell Therapy for Esophageal Anastomotic Leakage by Autografting Stromal Cells in Fibrin Scaffold

XIANG XUE <sup>a</sup>, YAN YAN,<sup>b</sup> YE MA,<sup>c</sup> YANG YUAN,<sup>c</sup> CHUNGUANG LI,<sup>c</sup> XILONG LANG,<sup>c</sup> ZHIYUN XU,<sup>c</sup> HEZHONG CHEN,<sup>c</sup> HAO ZHANG<sup>c</sup>

**Key Words.** Esophageal anastomotic leakage • Mesenchymal stromal cells • Fibrin scaffold • Autograft

<sup>a</sup>Division of Cardiothoracic Surgery, The Second Affiliated Hospital, Soochow University, Suzhou, People's Republic of China;

<sup>b</sup>Cardiovascular Therapeutic Center, No. 117 Hospital of Chinese People's Liberation Army, Hangzhou, People's Republic of China; <sup>c</sup>Institute of Cardiothoracic Surgery at Changhai Hospital, Second Military Medical University, Shanghai, People's Republic of China

Correspondence: Hao Zhang, M.D., Institute of Cardiothoracic Surgery at Changhai Hospital, Second Military Medical University, Shanghai 200433, People's Republic of China. Telephone: 86-13818178916; e-mail: dr\_zhanghao@126.com

Received June 21, 2018; accepted for publication December 4, 2018; first published February 27, 2019.

<http://dx.doi.org/10.1002/sctm.18-0137>

This is an open access article under the terms of the Creative Commons Attribution-NonCommercial-NoDerivs License, which permits use and distribution in any medium, provided the original work is properly cited, the use is non-commercial and no modifications or adaptations are made.

### ABSTRACT

Esophageal anastomotic leakage (EAL) is a devastating complication for esophagectomy but the available therapies are unsatisfactory. Due to the healing effects of mesenchymal stromal cells (MSCs) and supporting capability of fibrin scaffold (FS), we evaluated the efficacy of a stem-cell therapy for EAL by engrafting adult and autologous MSCs (AAMSCs) in FS and investigated the potential mechanism. Twenty-one rabbits were assigned to AAMSC/FS group ( $n = 12$ ) and control group ( $n = 9$ ). After harvested, AAMSCs were identified and then labeled with lenti.GFP. To construct EAL model, a polyethylene tube was indwelled through the anastomosis for 1 week. A total of  $2 \times 10^6$  AAMSCs in 0.2 ml FS were engrafted onto the EAL for the AAMSC/FS group, whereas FS was injected for control. Magnetic Resonance Imaging (MRI) examination was performed after 5 weeks. Esophageal tissues were harvested for macroscopic, histological analyses, Western blot, and immunohistochemistry at 8 weeks. The animal model of EAL was established successfully. MRI scanning revealed a decreased inflammation reaction in AAMSC/FS group. Accordingly, AAMSC/FS group presented a higher closure rate (83.3% vs. 11.1%,  $p = .02$ ) and lower infection rate (33.3% vs. 88.9%,  $p = .02$ ). Histological analyses showed the autografted MSCs resided in the injection site. Furthermore, milder inflammation responses and less collagen deposition were observed in AAMSC/FS group. Western blot and immunohistochemistry studies suggested that the therapeutic effect might be related to the secretions of IL-10 and MMP-9. Engrafting AAMSCs in FS could be a promising therapeutic strategy for the treatment of EAL by suppressing inflammation response and alleviating fibrosis progression. *STEM CELLS TRANSLATIONAL MEDICINE* 2019;8:548–556

### SIGNIFICANCE STATEMENT

For future applications in clinical practice, the autografting of mesenchymal stromal cells in fibrin scaffold could be used concomitantly with the esophagectomy to prevent the occurrence of esophageal anastomotic leakage, thus improving the surgical outcome for esophageal cancer. In addition, the proposed approach would be used to close or repair various leakages and fistulas, such as tracheoesophageal fistula, intestinal fistula, and even the incision of natural orifice transluminal endoscopic surgery (NOTES) through an endoscope. Therefore, the present approach provides a promising alternative for the treatment of several gastroenterological diseases in future clinical practice.

### INTRODUCTION

Esophagectomy is the mainstay of curative treatment for locoregional esophageal cancer with or without chemo/radiotherapy [1]. Despite of improvements in surgical technique and postoperative care, esophageal anastomotic leakage (EAL) remains one of the most devastating complications after esophagectomy with a reported incidence up to 35% [2]. EAL could lead to mediastinitis and pyothorax during postoperative

period and therefore significantly increases the postoperative morbidity and mortality. Recent research reported that EAL could also adversely impact the long-term survival and induce the recurrence of locoregional cancer [3]. Conservative strategies including drainage, anti-infection treatment, and even aggressive surgical repair are not yet satisfactory for the treatment of EAL.

Mesenchymal stromal cells (MSCs), defined as possessing the capacity for multilineage differentiation, are potential candidates for replacement

of damaged tissues [4]. In recent years, there are increasing interests in manipulation of MSCs as a regenerative therapy for various diseases, such as myocardial infarction [5], spinal cord injury [6], liver cirrhosis [7], gastric perforation [8], broncho-pneural leakage [9], penetrating ulcers [10], and Colitis [11]. Furthermore, the manipulation of adult and autologous MSCs (AAMSCs) is particularly promising, which could improve the endogenous regenerative potential without risks of rejection or ethical issues related to heterologous or homologous stem cell transplantation [12]. These potential benefits of AAMSCs provide the possibility for the therapy of EAL. However, migration and death of the implanted MSCs has been widely reported to decrease the therapeutic effect in several studies [13, 14]. In recent years, fibrin has been demonstrated with the potential of supporting long-term survival and proliferation of MSCs through specific homing and in situ cell retention, and therefore enhances the therapy efficacy of MSC transplantation [15].

For these reasons, we hypothesized that engrafting AAMSCs in fibrin scaffold (FS) could provide a promising therapy for EAL. The efficacy and underlying mechanisms of this strategy were investigated in this work.

## MATERIALS AND METHODS

### Animals

The healthy adult male New Zealand rabbits aged to 12 months were purchased from the animal center of Second Military Medicine University. The animals were maintained under specific pathogen-free condition in accordance with ethical guidelines for the care of the Laboratory Animals of Changhai Hospital. This study was approved by the Committee of Changhai Hospital on the Use and Care of Animals (CHEC-2014-0015).

### AAMSCs Preparation

A total of 21 rabbits were randomly assigned to the AAMSC/FS group ( $n = 12$ ) and control group ( $n = 9$ ). For the preparation of AAMSCs, 1 ml bone marrow was aspirated from the tibia of each animal after anesthetization. Then the AAMSCs were isolated by Ficoll-paque density gradient, plated in 6 well cell culture plates and incubated ( $37^{\circ}\text{C}$ , 5%  $\text{CO}_2$ ) in Dulbecco's modified Eagle's medium (DMEM, Gibco, Grand Island, NY, <https://www.thermofisher.com/>) containing 1% penicillin-streptomycin (Sigma-Aldrich, St. Louis, MO, <https://www.sigmaaldrich.com/>) and 20% fetal bovine serum (FBS, Gibco) for 14 days as primary culture. The mediums were exchanged every 2 days. MSC-specific cell surface markers were identified by flow cytometry for the cultured cells. Briefly, the cells were incubated with Mouse Mesenchymal Stromal Cell Marker antibodies (1:100, Abcam, Cambridge, U.K., <http://www.abcam.com/>) for CD29, CD44, CD90, and CD45 for 1 hour at room temperature. After being washed to remove unbound primary antibodies, the cells were incubated for 30 minutes with goat anti-chicken Alexa fluor-488 conjugated secondary antibody (1:100, Jackson Laboratory Bar Harbor, ME, <https://www.jax.org/>) and then analyzed on a flow cytometry (Miltenyi Biotec, Bergisch Gladbach, Germany, <https://www.miltenyibiotec.com/CN-en/>) with the FlowJo software (Tree Star Inc., <https://www.flowjo.com/>).

The adipogenic and osteogenic differentiation was induced with adipogenesis medium (Gibco) for 14 days and osteogenesis medium (Gibco) for 28 days, respectively. The differentiation

into adipocyte or osteocytes was respectively confirmed by staining with oil-red O or alizarin red. For in vivo tracing, the AAMSCs were transfected with lenti.GFP (MOI: 40 TU per cell) under normal growth condition for 6 hours. The third passage of spindle-shaped GFP<sup>+</sup>-MSCs were used for autograft.

### EAL Model Construction

For each animal, the cervical esophagus was isolated, transected and anastomosed with a 2 mm leakage left. Then a polyethylene tube (2.4 mm caliber) was put through the leakage to create EAL with its inlet left in the esophageal lumen and the outlet was left outside the cervical skin for 1 week (Fig. 1A, 1B). After the surgery, oral intake was stopped and enteral nutrition was fed via the indwelling polyethylene tube for all animals. Broad spectrum antibiotic treatment was administered intravenously. One week after the model construction, the sutures of cervical incisions were taken out and the polyethylene tube was removed. The EAL was carefully exposed and the caliber of EAL was measured (Fig. 1C).

### Engrafting AAMSCs in FS to EAL

The FS was prepared prior to engraftment as following. In brief, the lyophilized fibrinogen was mixed with 2 ml dilution buffer. Then a total of 2 ml of 40 mmol/l  $\text{CaCl}_2$  solution was added to 500 IU/ml thrombin. The 2 solutions were mixed 1:1 to resemble the FS through a Y-shape syringe during the procedure of engraftment (Fig. 2D). A total of  $2 \times 10^6$  AAMSCs in 0.2 ml FS were injected onto EAL for each of the animals in AAMSC/FS group, whereas 0.2 ml FS alone was injected for animal in control group. Afterward, the cervical incisions were closed by running suturing. All animals were fed through a stomach tube after the procedure.

### Cervical Magnetic Resonance Imaging Evaluation

Five weeks after the treatment, all the animals underwent cervical Magnetic Resonance Imaging (MRI) scanning to evaluate the focal status of EAL by using 3.0 T superconducting MRI scanner (Toshiba, Tokyo, Japan, <http://www.toshiba.co.jp/worldwide/>). All the images were reviewed and interpreted by 2 senior radiologists, and the analysis were performed under standard procedure, the radiologists were blinded for analysis. Horizontal T2-weighted images were obtained using following settings: spin-echo sequence: T2WI, time of repetition: 702 seconds, time of echo: 17 seconds, field of view: 320 mm  $\times$  320 mm and section thickness: 5 mm.

### Histological Analyses

The animals were sacrificed at the end time of the study (8 weeks after the treatment). The gross specimens of esophagi at EALs were harvested and inspected carefully formacroscopic investigation. The calibers of unclosed EALs were measured. Then the specimens were fixed with 10% buffered formaldehyde, dehydrated with a series of graded ethanol and embedded in paraffin. Specimens were sliced into 4  $\mu\text{m}$  thick sections for histological analyses with hematoxylin-eosin (H&E) and Van Gieson (VG) staining. Microscopic examinations were performed under light microscope (Olympus, Japan, <https://www.olympus-global.com/>) and photographed by microscopy imaging system (Olympus).

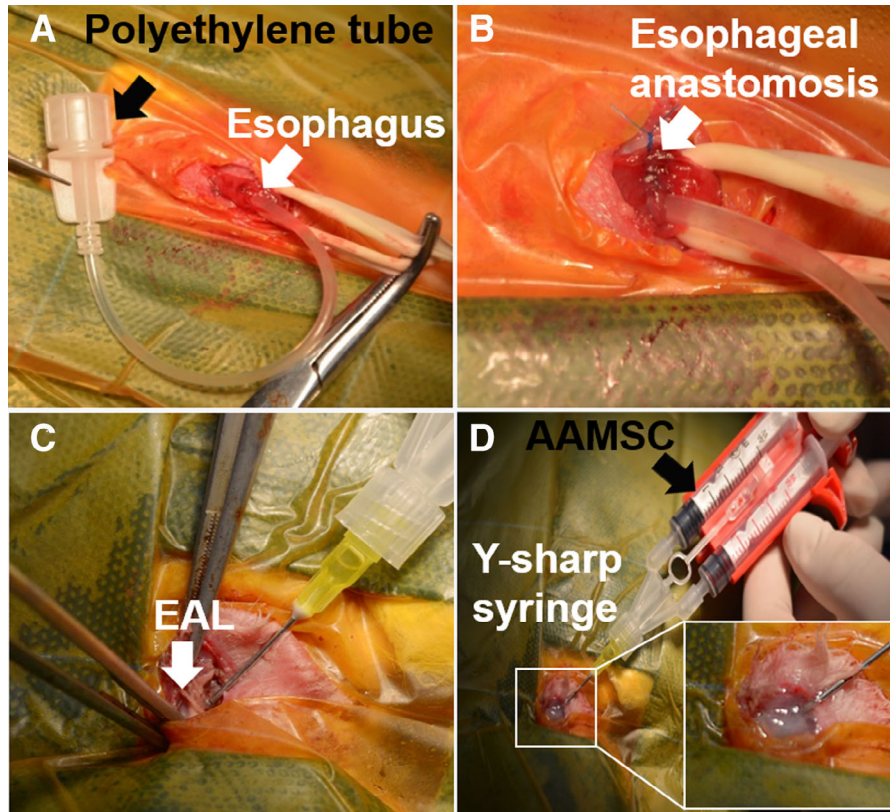


**Figure 1.** The establishment of animal model of EAL and engraftment of AAMSCs in FS. **(A):** After the esophagectomy, a polyethylene tube was inserted into the esophagus and served as a feeding tube. **(B):** Esophageal anastomosis was performed with the polyethylene tube left inside the esophageal lumen and fixed. **(C):** The polyethylene tube was removed and the EAL was exposed 1 week later. **(D):** The AAMSCs in FS were injected onto the leakage with a Y-shape syringe for AAMSC/FS group (the injected AAMSCs in FS were shown in the enlarged panel), while the same procedures were performed with FS alone for control group. Abbreviations: EAL, esophageal anastomotic leakage; AAMSCs, adult and autologous mesenchymal stromal cells; FS, fibrin scaffold.

### Immunofluorescence Study

Immunofluorescence staining of GFP and  $\alpha$ -SMA was carried out for tracing the biological behavior of engrafted GFP<sup>+</sup>-AAMSCs in vivo. Briefly, after dewaxing, rehydration, antigen retrieval and blocking, the sections were incubated with mouse anti  $\alpha$ -SMA and GFP antibodies (1:50, Abcam), respectively, overnight at 4°C. Sections were then incubated with the goat anti-mouse Alexa-594 conjugated secondary antibody (1:500, Jackson Laboratory) and the goat anti-chicken Alexa-488 conjugated secondary antibody (1:500, Jackson Laboratory) for 1 hour. Finally, the nuclei were counterstained with DAPI (1:10,000, Beyotime, Shanghai, China, <http://www.beyotime.com/index.html>).

### Cytokine Expression Assays

The primary antibodies used were anti TNF- $\alpha$ , TGF- $\beta$ , IL-6, IL-10, MMP-2, MMP-9, HSP47, VEGF, Collagen-I (Abcam). All primary antibodies were used at dilution 1:100 for Western blot (WB) analyses and 1:50 for the immunohistochemistry study.

For WB analyses, total proteins were extracted from the tissues in EALs and the concentrations were measured using the Enhanced Bicinchoninic Acid Protein Assay Kit (Beyotime, China). Thirty micrograms of the proteins were loaded into each well on 10% SDS-polyacrylamide gels and then transferred to PVDF membranes (Millipore, Billerica, MA). The membranes were blocked with 5% skim milk solution for 1 hour at room

temperature and incubated with primary antibody and anti- $\beta$ -actin antibody (1:10,000, Protein Tech, <https://www.ptglab.com/>) overnight at 4°C. After being washed three times in 0.2% TBS-Tween, the membranes were incubated for 1 hour with HRP-conjugated secondary antibody. Finally, the blot was developed using the substrate (Thermo Fisher, Massachusetts, <https://www.thermofisher.com/>). The protein bands were quantified using Image J software (National Institutes of Health, Bethesda, Maryland, <https://imagej.nih.gov/>).

For the immunohistochemistry studies, the sections were firstly deparaffinized and rehydrated. Endogenous peroxidase was then quenched using 10% H<sub>2</sub>O<sub>2</sub> for 10 minutes at room temperature. Subsequently, excess proteins were blocked with 10% goat serum for 1 hour. The sections were respectively incubated with the primary antibodies as mentioned above overnight at 4°C. Afterward, the sections were rinsed and incubated with biotin-labeled goat anti-mouse IgG. The DAB Horseradish Peroxidase Color Development Kit (Beyotime) was used for color development. Finally, the sections were counterstained with hematoxylin and mounted.

### Statistics

All statistical analyses were performed with GraphPad Prism 6 (GraphPad Software, Inc., CA, <https://www.graphpad.com/>). A *p* value of less than .05 was considered significant. All parametric

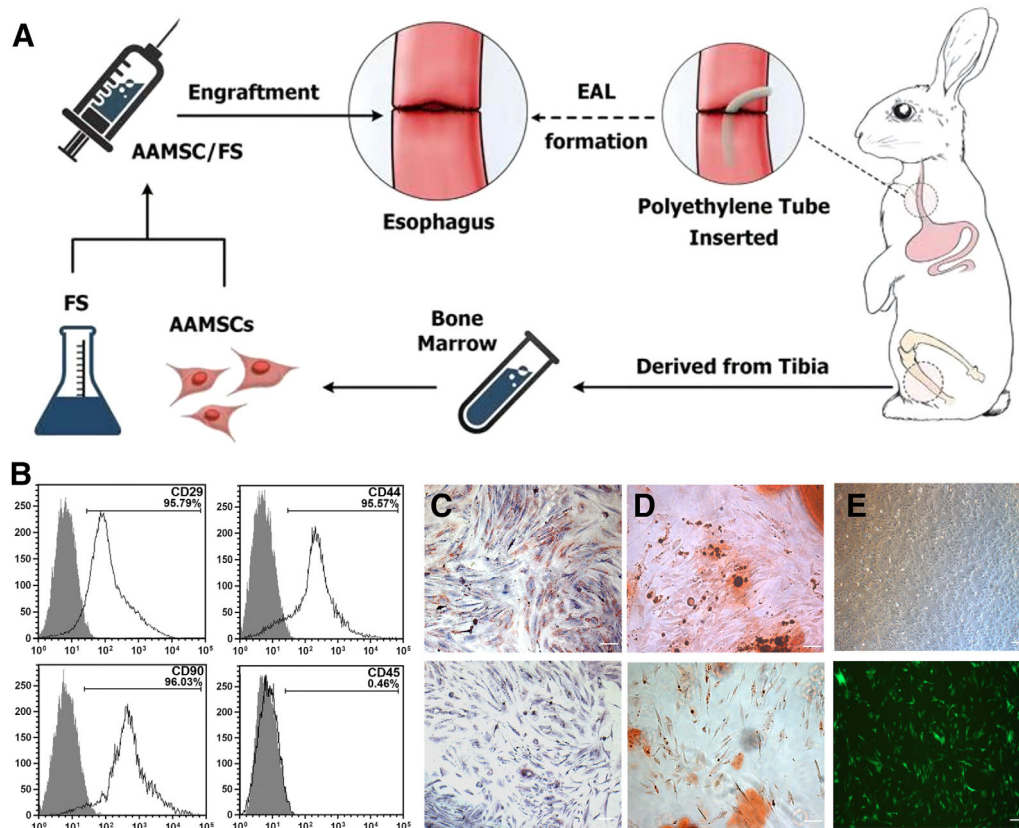


**Figure 2.** The schematic diagram and characterizations of the cultured AAMSCs in vitro. **(A):** Schematic representation of our study. The AAMSCs derived from bone marrow of the animal were engrafted in FS for the treatment of the EAL. **(B):** Cell-surface markers of AAMSCs were assessed by flow cytometry showing the strong expressions of CD29, CD44, CD90, and lack of CD45 in AAMSCs. **(C):** Adipogenesis was demonstrated by the accumulation of neutral lipid vacuoles that stained by oil red O (upper panel) with negative control (lower panel). Scale bar: 100  $\mu$ m. **(D):** Osteogenesis was demonstrated by the calcium deposition that stained by alizarin red (upper panel) with negative control (lower panel). Scale bar: 100  $\mu$ m. **(E):** Microscopy examination of AAMSCs transfected by lenti.GFP showed that spindle-shaped AAMSCs approach 80% confluent on 6 well cell culture plate. Scale bar: 200  $\mu$ m. **(F):** Fluorescence microscopy examination of the same clone revealed that  $\sim$ 60% of AAMSCs expressed GFP. Scale bar: 200  $\mu$ m. Abbreviations: AAMSCs, adult and autologous mesenchymal stromal cells; FS, fibrin scaffold; EAL, esophageal anastomotic leakage; GFP, green fluorescent protein.

statistical tests met the assumptions of the tests (normal distribution or equal variance). Quantitative datum were represented as mean  $\pm$  SD. Two-tailed Student's *t* test was performed to analyze the results of quantitative data and Fisher exact *t* test was used to compare differences of rates. The survival curve was analyzed with the methods of Kaplan–Meier and the comparisons between 2 groups were made with log-rank test.

## RESULTS

### Characteristics of AAMSCs

The schematic diagram of the current work was illustrated in Figure 1A. The spindle-shaped third passage AAMSCs were plated at  $5 \times 10^5$  densities in 20% DMEM on cell culture plates. MSC-specific cell surface markers CD29, CD44, and CD90 strongly expressed in AAMSCs, whereas hematopoietic marker CD45 was negative (Fig. 2B). Furthermore, differentiation assays showed the positive staining of oil red O and alizarin red (Fig. 2C, 2D), indicating the differentiation of AAMSCs toward adipocytes and osteoblasts, respectively. Ten days after the transfection of lenti.GFP, the spindle shaped third passage AAMSCs approached 80% confluence on 6 well cell culture

plates and the green fluorescence could be observed in  $\sim$ 60% of the cells with inverted fluorescence microscopy (Fig. 2E, 2F).

### Animal Model of EAL

One week after the construction for the animal model, the EALs could be observed in all the animals. The rabbits were identified as suffering with localized infection, if they had obvious signs of redness, swelling, purulent drainage around the EAL, or abnormal temperature. The calibers of EALs were  $2.3 \text{ mm} \pm 0.15 \text{ mm}$  ( $n = 12$ ) for AAMSC/FS group and  $2.2 \text{ mm} \pm 0.17 \text{ mm}$  ( $n = 9$ ) for control group, respectively ( $p > .05$ ). Meanwhile, there was no significant difference between groups in localized infection around EALs (15.7% vs. 11.1%,  $p > .05$ ).

### Clinical Outcomes

Five weeks after the treatment, narrowed and localized high-intensity signals were observed by cervical MRI evaluation in the animals of AAMSC/FS group. In contrast, mass of high-intensity signals and tracheal deviation could be found in control animals, indicating severe focal abscess formed (Fig. 3A). In the control group, 88.9% of the rabbits showed high signal intensity, whereas only 25% in the AAMSC/FS group ( $p = .008$ ). The gross specimens of esophagi at EALs were harvested at

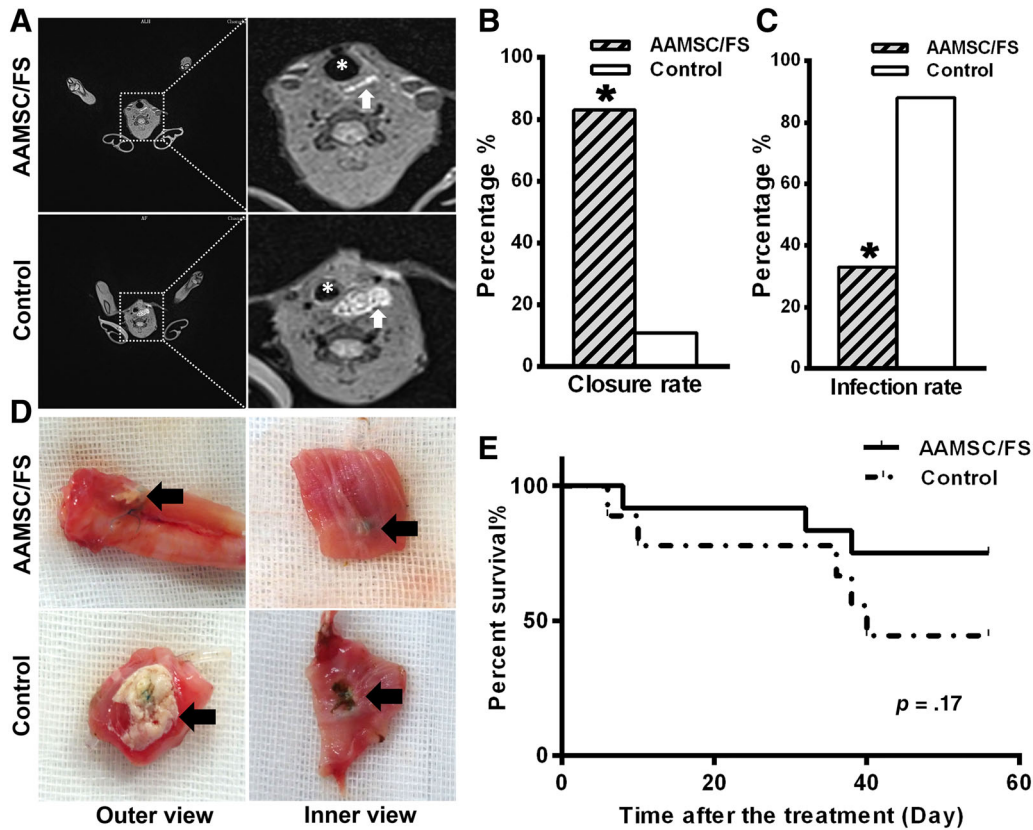


**Figure 3.** Representative images of cervical MRI and gross specimens, and clinical outcomes. **(A):** Representative images of follow-up cervical MRI after 5 weeks of the treatment showed that there was only a linear of high intensity in front of esophagus on T2-weighted images in AAMSC/FS group, meanwhile, there was mass of high signal intensity between esophagus and main bronchus and the bronchus was deviated from midline in control group. White arrow: esophagus; white asterisk: main bronchus. **(B, C):** Rates of closure and infection in 2 groups. There was a significant difference. \* $p = .02$ , Fisher exact  $t$  test. **(D):** Representative images of gross specimens of esophageal tissue around EALs showed that the EALs of AAMSC/FS group were completely occluded with both mucosal and adventitial healing. By contrast, the EALs in control group persistently existed with white purulent secretion on the adventitia layer. Black arrow: EAL. **(E):** Percent of survival showed that the risk of fatal outcome of control group was twice higher than AAMSC/FS group, however, no significant difference was detected between the 2 groups;  $p = .17$ , log-rank test. Abbreviations: MRI, magnetic resonance imaging; AAMSCs, adult and autologous mesenchymal stromal cells; FS, fibrin scaffold; EAL, esophageal anastomotic leakage.

the end time of the study (8 weeks after the treatment). The closure of ELA was regarded as the mucosal layer occlusion and no signs of leakage such presence of abscess and formation of sinus. Macroscopic investigation suggested that EALs were occluded in 10 of 12 animals in AAMSC/FS group (83.3%) and 1 of 9 animals in control group (11.1%;  $p = .02$ ; Fig. 3B). In addition, the infection rate was 33.3% (4/12) for AAMSC/FS group compared with 88.9% (8/9) for control with a significant difference ( $p = .02$ ; Fig. 3C). The representative photographs of esophageal specimens at EALs were shown in Figure 3D for both groups.

In AAMSC/FS group, 3 of 12 rabbits died of sepsis caused by uncontrolled infection. Meanwhile, of the total 9 rabbits in control group, 5 died during the follow-up period. The causes of death were severe sepsis in 4 rabbits and respiratory failure induced by esophago-tracheal leakage in 1 rabbit. However, there was no significant difference for the mortality between the 2 groups (25.0% vs. 55.9%,  $p = 0.17$ ; Fig. 3E).

#### Focal Inflammation Response and Fibrosis Progression

For animals in AAMSC/FS group with closed EALs, the H&E staining of esophagi at EALs showed dispersive inflammatory cells

infiltration and VG staining revealed that the red-stained collagen fibers were sparse and regularly organized. In contrast, severe signs of the inflammation response could be observed for control group, such as diffuse infiltration of inflammatory cells, and aggravated proliferation of the adjacent tissues (Fig. 4A). Furthermore, collagen deposition between submucosa layer and muscular layer was heavier and the collagen fibers distributed compactly and disorderly.

#### Fate of Engrafted AAMSCs

In AAMSC/FS group, GFP<sup>+</sup>-AAMSCs could be identified from the submucosa of esophageal wall at EALs by immunofluorescence study, indicated that engrafted AAMSCs resided in the site of injection after 8 weeks of engraftment, as shown in Figure 4B.

Interestingly, the expression of  $\alpha$ -SMA (red), which was a reliable biomarker of myofibroblasts, could be simultaneously observed with the engrafted AAMSCs (green) at EALs.

#### Autografted MSCs Mediate Paracrine Action

Our results of WB analyses and immunohistochemistry study revealed that compared with control group, the expressions

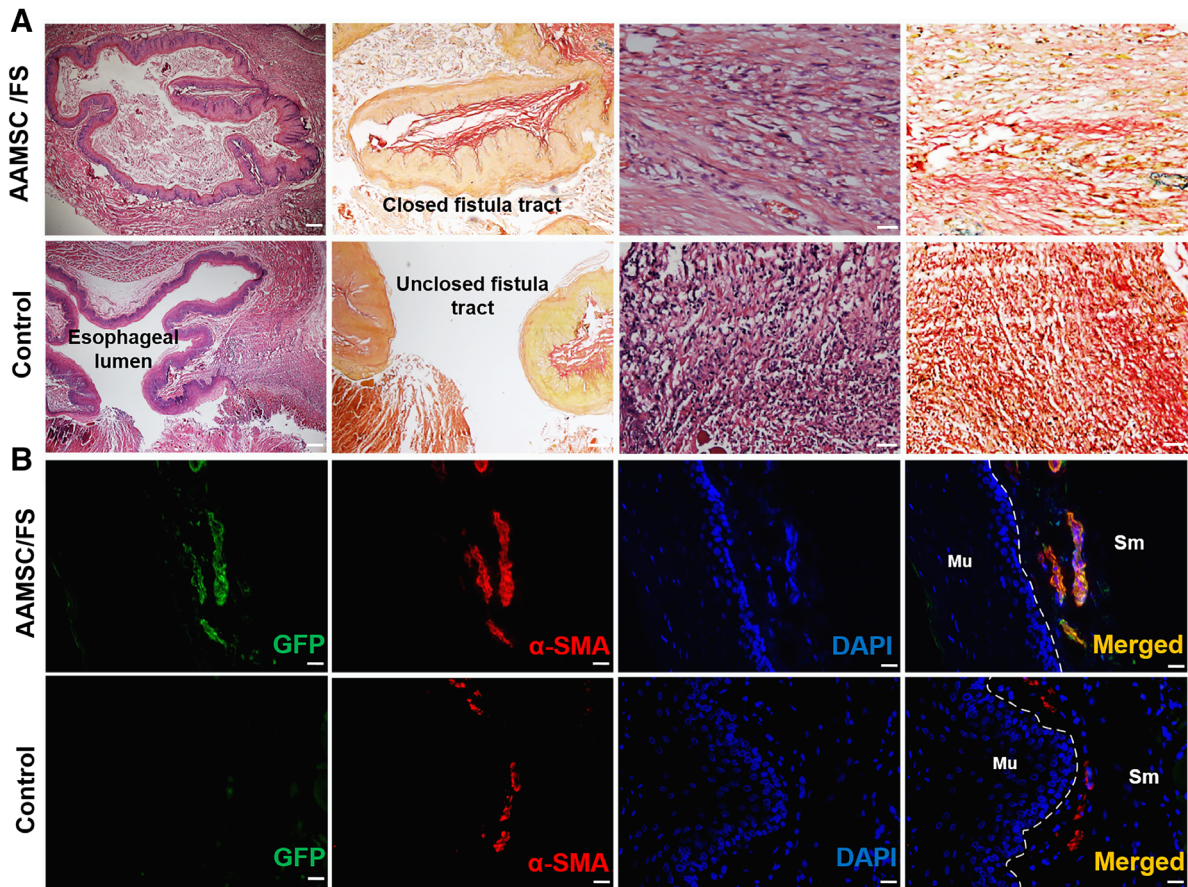


**Figure 4.** Representative histological (hematoxylin-eosin and Van Gieson staining) and immunofluorescence images of esophageal wall at EALs after 8 weeks of the treatment (cross sections). **(A):** Dispersive inflammatory cells infiltrated in the tissue adjacent to EAL in AAMSC/FS group. The collagen fibers were sparse and regularly organized (upper panel). However, diffuse infiltration of inflammatory cells, and aggravated proliferation could be observed for control group. Furthermore, collagen deposition between submucosa layer and muscular layer was heavier and the collagen fibers distributed compactly and disorderly (lower panel). Scale bars: 200  $\mu\text{m}$  (left-most). Scale bar: 50  $\mu\text{m}$  (right panel). **(B):** Immunofluorescence staining of the esophageal wall at EALs demonstrated that the engrafted AAMSCs were positive for anti-GFP expression (green) and anti- $\alpha$ -SMA antigen (red). Nuclei were counterstained with DAPI (blue). Colocalization of anti- $\alpha$ -SMA antigen and anti-GFP antigen were seen as yellow. Scale bars: 20  $\mu\text{m}$ . Abbreviations: AAMSCs, adult and autologous mesenchymal stromal cells; EAL, esophageal anastomotic leakage; FS, fibrin scaffold; GFP, green fluorescent protein;  $\alpha$ -SMA,  $\alpha$  smooth muscle actin; DAPI, 4',6-diamidino-2-phenylindole; Sm, submucosa; mu, mucous layer.

of IL-10 and MMP-9 were significantly increased, whereas the expressions of TNF- $\alpha$  and TGF- $\beta$  were significantly decreased after the engraftment of AAMSCs in FS, as shown in Figure 5A. The representative images were shown in Figure 5B, 5C. These evidences strongly suggest that the suppressing effects on inflammatory response and fibrosis progression might be mediated through the paracrine action of the engrafted AAMSCs.

## DISCUSSION

EAL is one of the most frequent and troublesome postoperative complications after esophagectomy for patients with esophageal cancer [16, 17]. It may cause mediastinitis or pyothorax in early postoperative period and prolong the hospital stay. Conservative strategies including adequate drainage and infection control or even aggressive surgical repair for the treatment of EAL are not yet satisfactory [18]. In recent years, MSC transplantation has proved to be a promising strategy in cell therapy and regenerative medicine for various diseases and numerous clinical applications are under study in ischemic heart disease,

atherosclerosis, stroke, diabetes, and organ's reconstruction [19]. In the present study, we for the first time explored the application of adult and autologous MSCs (AAMSCs) for the treatment of EAL. To evaluate the therapeutic effect of this approach, the animal model of EAL should be established first. However, to the best of our knowledge, it has not been proposed and reported as of now. Hence, we developed a method in the current study to establish the animal model of EAL with the adult rabbit by indwelling a polyethylene tube through the anastomosis to create a predictable EAL. At the time for engraftment, EALs could be identified in all the animals and no significant difference was detected in the calibers of leakages and infection rate between 2 groups. In this regard, we consider that the proposed method provides an effective and reliable way for the construction of the animal model of EAL and the established model is suitable for the evaluation of therapeutic effect on EAL.

The most common routes for MSC transplantation are systemic (intravenous) and local injection. Local injection offers more cells in targets site than systemic injection, but the migration and death of implanted MSCs decreased the viable cells at the target site [20]. Fibrin has been demonstrated to be

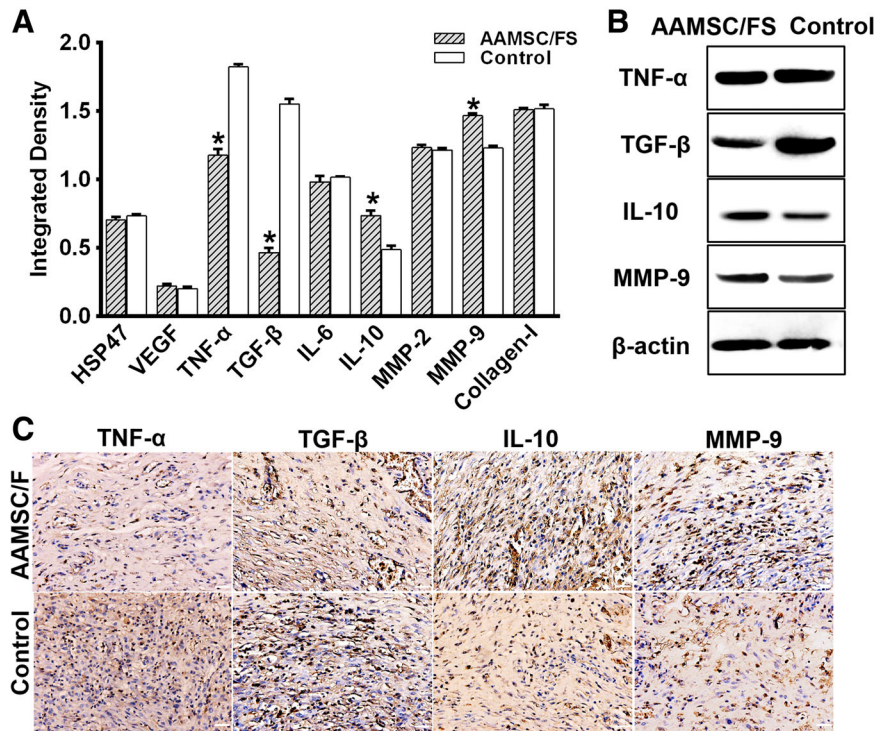


**Figure 5.** Evidence of WB analyses and immunohistochemistry staining. **(A):** Quantitative analyses of Western blot (WB) showed that increased expressions of TNF- $\alpha$ , TGF- $\beta$  and decreased expressions of IL-10, MMP-9 in AAMSC/FS group. However, there were no significant differences of expressions of HSP47, VEGF, IL-6, MMP-2, and collagen-I between the 2 groups. Mean  $\pm$  SEM; \*,  $p < .05$ , two-tailed Student's  $t$  test. **(B):** Representative photos from WB analyses of TNF- $\alpha$ , TGF- $\beta$ , IL-10, MMP-9, with  $\beta$ -actin as internal control, showing that engraftment of AAMSCs in FS could decrease the protein expressions of TNF- $\alpha$ , TGF- $\beta$  and increase the expressions of IL-10 and MMP-9. **(C):** Representative images of immunohistochemistry studies showing the same expression changes of TNF- $\alpha$ , TGF- $\beta$ , IL-10, and MMP-9 throughout the serosal layer and muscular layer. Scale bar: 50  $\mu$ m. Abbreviations: WB, Western blot; TNF- $\alpha$ , tumor necrosis factor- $\alpha$ ; TGF- $\beta$ , transforming growth factor- $\beta$ ; IL-10, Interleukin-10; MMP-9, matrix metalloproteinase-9; AAMSCs, adult and autologous mesenchymal stromal cells; FS, fibrin scaffold.

capable of facilitating MSCs retention, survival, proliferation, and differentiation [21, 22]. The reason might be the suitable matrix environment provided by its three-dimensional structure, such as temporary retention space, cytoprotective effects and cell-matrix interactions [23]. Furthermore, fibrin could be biodegraded by plasmin *in vivo* within 1–2 weeks and then eliminated by the kidneys without toxic residue [24]. Thus, we employed fibrin as the scaffold to sustain the autografted MSCs in this study to induce a synergistic effect for the treatment of EAL.

After 8 weeks of autografting MSCs in FS, the GFP<sup>+</sup>-MSCs could be found and identified in the esophageal wall around EAL by immunofluorescence study, suggesting that the autografted MSCs survived and resided in the implantation site. Moreover, interestingly, the GFP<sup>+</sup>-MSCs were also positive for  $\alpha$ -SMA (Fig. 4B, lower panel) which is a reliable biomarker for myofibroblasts [25]. We inferred 2 mechanisms that contribute to the EALs healing process: one of possible mechanism may be related to differentiation potential of the AAMSCs; the other was that AAMSCs may stimulate the transdifferentiation of other cells around EALs to myofibroblasts.

The histological analyses revealed that the inflammation response and fibrosis was milder in AAMSC/FS group than control, indicating the autografted MSCs in FS could attenuate the inflammation response and fibrosis progression. Many previous studies implicated that MSCs exerted the tissue repair function by synthesizing and secreting a broad spectrum of cytokines and chemokines on cells in their vicinity [26, 27]. To investigate

the underlying mechanism for the healing effects of autografting MSCs in FS on EAL, immunohistochemistry studies and WB analyses were performed in the present study. Our results revealed the upregulation of IL-10 and MMP-9, whereas downregulation of TNF- $\alpha$  and TGF- $\beta$  after autograft of MSCs in FS. The 4 cytokines have been widely demonstrated to be involved in the paracrine function of MSCs [28–32]. Specifically, IL-10 is a well-known anti-inflammatory cytokine that can inhibit the secretion of proinflammatory cytokines, such as IL-2, IL6, TNF- $\alpha$ , and TGF- $\beta$  [31, 32]. MMP-9, are one family of enzymes which are capable to digest collagen and promote extracellular matrix (ECM) degradation in tissue repair process [33]. In contrast, TNF- $\alpha$  is considered to be a strong proinflammatory cytokine which could initiate the cascade of proinflammatory cytokines through enhancing activation of the NF- $\kappa$ B signaling pathway [30]. TGF- $\beta$  a role in all phases of tissue repair process and one of the most important functions of TGF- $\beta$  is chemotactic availability, enabling it to recruit fibroblasts and immune cells such as macrophages, monocytes, and T-cells [34, 35]. The downregulation of TNF- $\alpha$  and TGF- $\beta$  might be related with the inhibiting function of IL-10 which has been verified in several studies. Taken together, these evidences strongly suggest that the suppressing effects on inflammatory response and fibrosis progression around EAL might be mediated through the paracrine pathway of the autografted MSCs in FS.

In addition, a clearly higher closure rate of EAL was achieved in AAMSC/FS group than control group (83.3% vs. 11.1%).

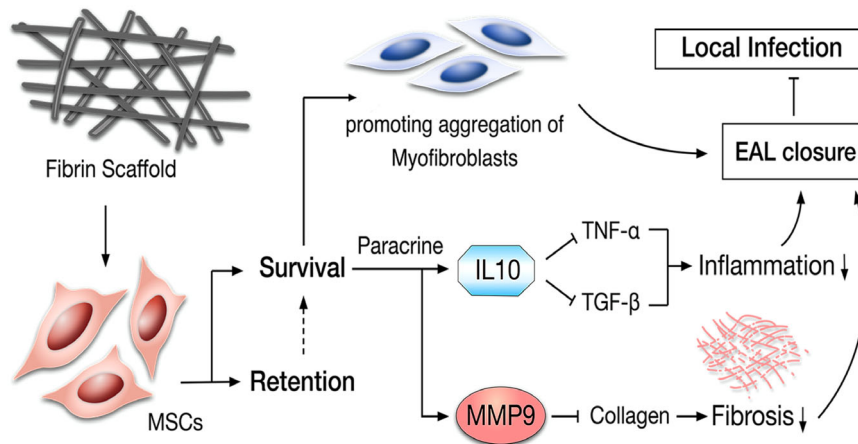


**Figure 6.** Schematic overview of active roles of AAMSCs in FS in the treatment of esophageal anastomotic leakage. Due to the FS, AAMSCs were survived and retained after autografted onto EAL for 8 weeks, the autografted MSCs have differentiation potential, they may differentiate to myofibroblasts to replace the damaged tissue or AAMSCs stimulate the transdifferentiation of other cells around EALs to myofibroblasts. In addition, AAMSCs in FS aggregates remain in the site of injection, increasing the expression of IL-10, a potent anti-inflammation cytokine, which reduces the expression of proinflammation mediator such as TNF- $\alpha$ , TGF- $\beta$ , meanwhile, enhancing the expression of MMP-9, which inhibits the deposition of collagen and alleviates the fibrosis progression through a paracrine mechanism. Thus, promoting the closure of EAL and alleviating the local infection. Abbreviations: AAMSCs, adult and autologous mesenchymal stromal cells; FS, fibrin scaffold; EAL, esophageal anastomotic leakage; IL-10, Interleukin-10; TNF- $\alpha$ , tumor necrosis factor- $\alpha$ ; TGF- $\beta$ , transforming growth factor- $\beta$ ; MMP-9, matrix metalloproteinase-9.

Moreover, the infection rate of AAMSC/FS group was lower than control (33.3% vs. 88.9%). We refer that the alleviated inflammation and fibrosis improved the tissue regeneration around EAL and promoted the closure of EAL in AAMSC/FS group. The decreased infection rate might be also contributed to the closure of EAL. It has been reported that MSCs could attenuate infection via inhibiting the overproduction of prostaglandin and recruitment of macrophages [36].

Furthermore, the survival rate of AAMSC/FS group was more than twice higher than control group (55.9% vs. 25%), although no statistic difference in mortality was detected between the 2 groups. All these results suggested that autografting of MSCs in FS provide a superior healing effect on the therapy of EAL.

## CONCLUSION

With the supporting of FS, adult and autologous MSCs could promote the healing effect of EAL by attenuating the inflammatory response and fibrosis through their paracrine pathway (Fig. 6), which can be pursued as a novel and efficient.

## CLINICAL PROSPECTIVE

For future application in clinical practice, the autografting of MSCs in FS could be used concomitantly with the esophagectomy to prevent the occurrence of EAL, thus improve the surgical outcome for esophageal cancer. In addition, the proposed approach would be used to close or repair various leakages

and fistulas, such as tracheoesophageal fistula, intestinal fistula and even the incision of natural orifice transluminal endoscopic surgery (NOTES) through an endoscope. Therefore, the present approach provides a promising alternative for the treatment of several gastroenterological diseases in future clinical practice.

## ACKNOWLEDGMENTS

This work was supported by the National Natural Science Foundation of China (Grant Nos. 81271707, 81371692, and 30700157).

## AUTHOR CONTRIBUTIONS

X.X., Y.Y., Y.M.: contributed equally to this work as first authors; X.X., Y.Y., Y.M.: performed the experiments, drafted the manuscript; Y.Y., C.G.L.: provided critical research resources and consultation; X.L.L.: collected, analyzed and interpreted the data; H.Z.C., Z.Y.X.: developed the study hypothesis and designed the experiments; H.Z.: supported and supervised the study; X.X., Y.Y., Y.M., Y.Y., C.L., X.L., Z.X., H.C., H.Z.: read and approved the final manuscript.

## DISCLOSURE OF POTENTIAL CONFLICTS OF INTEREST

The authors indicated no potential conflicts of interest.

## REFERENCES

1 Abdel Aziz MT, Atta HM, Mahfouz S et al. Therapeutic potential of bone marrow-derived mesenchymal stem cells on experimental liver fibrosis. *Clin Biochem* 2007;40: 893–899.

2 Blencowe NS, Strong S, McNair AG et al. Reporting of short-term clinical outcomes after esophagectomy: A systematic review. *Ann Surg* 2012;255:658–666.

3 Markar S, Gronnier C, Duhamel A et al. The impact of severe anastomotic leak on long-term survival and cancer recurrence after

surgical resection for esophageal malignancy. *Ann Surg* 2015;262:972–980.

4 Hanson SE. Mesenchymal stem cells: A multimodality option for wound healing. *Adv Wound Care* 2012;1:153–158.

5 Chou SH, Lin SZ, Kuo WW et al. Mesenchymal stem cell insights: Prospects in



cardiovascular therapy. *Cell Transplant* 2014; 23:513–529.

6 Piltti KM, Salazar DL, Uchida N et al. Safety of human neural stem cell transplantation in chronic spinal cord injury. *STEM CELLS TRANSLATIONAL MEDICINE* 2013;2:961–974.

7 Puglisi MA, Tesori V, Lattanzi W et al. Therapeutic implications of mesenchymal stem cells in liver injury. *J Biomed Biotechnol* 2011; 2011:860578.

8 Caldas HC, de Paula Couto TA, Fernandes IM et al. Comparative effects of mesenchymal stem cell therapy in distinct stages of chronic renal failure. *Clin Exp Nephrol* 2015;19:783–789.

9 Petrella F, Spaggiari L, Acocella F et al. Airway fistula closure after stem-cell infusion. *N Engl J Med* 2015;372:96–97.

10 Liu L, Chiu PW, Lam PK et al. Effect of local injection of mesenchymal stem cells on healing of sutured gastric perforation in an experimental model. *Br J Surg* 2015;102: e158–e168.

11 Sala E, Genua M, Petti L et al. Mesenchymal stem cells reduce colitis in mice via release of TSG6, independently of their localization to the intestine. *Gastroenterology* 2015; 149:163–176.

12 Zhang H, Li S, Qu D et al. Autologous biological pacing function with adrenergic-responsiveness in porcine of complete heart block. *Int J Cardiol* 2013;168:3747–3751.

13 Nowacki M, Nazarewski L, Pokrywczynska M et al. Long-term influence of bone marrow-derived mesenchymal stem cells on liver ischemia-reperfusion injury in a rat model. *Ann Transplant* 2015;20:132–140.

14 Patel AN, Genovese J. Potential clinical applications of adult human mesenchymal stem cell (Prochymal[R]) therapy. *Stem Cells Cloning* 2011;4:61–72.

15 Barsotti MC, Felice F, Balbarini A et al. Fibrin as a scaffold for cardiac tissue engineering. *Biotechnol Appl Biochem* 2011;58:301–310.

16 Urschel JD. Esophagogastronomy anastomotic leaks complicating esophagectomy: A review. *Am J Surg* 1995;169:634–640.

17 Turkyilmaz A, Eroglu A, Aydin Y et al. The management of esophagogastric anastomotic leak after esophagectomy for esophageal carcinoma. *Dis Esophagus* 2009;22:119–126.

18 Nakajima M, Satomura H, Takahashi M et al. Effectiveness of sternocleidomastoid flap repair for cervical anastomotic leakage after esophageal reconstruction. *Dig Surg* 2014;31: 306–311.

19 Stoltz JF, de Isla N, Li YP et al. Stem cells and regenerative medicine: Myth or reality of the 21st century. *Stem Cells Int* 2015; 2015:734731.

20 Kim JE, Jung KM, Kim SH et al. Combined treatment with systemic and local delivery of substance P coupled with self-assembled peptides for a hind limb ischemia model. *Tissue Eng A* 2016;22:545–555.

21 Guo HD, Wang HJ, Tan YZ et al. Transplantation of marrow-derived cardiac stem cells carried in fibrin improves cardiac function after myocardial infarction. *Tissue Eng A* 2011;17:45–58.

22 Ho W, Tawil B, Dunn JC et al. The behavior of human mesenchymal stem cells in 3D fibrin clots: Dependence on fibrinogen concentration and clot structure. *Tissue Eng* 2006;12:1587–1595.

23 Ahmed TA, Ringuette R, Wallace VA et al. Autologous fibrin glue as an encapsulating scaffold for delivery of retinal progenitor cells. *Front Bioeng Biotechnol* 2014;2:85.

24 Kim I, Lee SK, Yoon JI et al. Fibrin glue improves the therapeutic effect of MSCs by sustaining survival and paracrine function. *Tissue Eng A* 2013;19:2373–2381.

25 Touhami A, Di Pascuale MA, Kawatika T et al. Characterisation of myofibroblasts in fibrovascular tissues of primary and recurrent pterygia. *Br J Ophthalmol* 2005;89:269–274.

26 Wu Y, Huang S, Enhe J et al. Bone marrow-derived mesenchymal stem cell attenuates skin fibrosis development in mice. *Int Wound J* 2014;11:701–710.

27 Wang M, Liang C, Hu H et al. Intraperitoneal injection (IP), intravenous injection

(IV) or anal injection (AI)? Best way for mesenchymal stem cells transplantation for colitis. *Sci Rep* 2016;6:30696.

28 Ueno T, Nakashima A, Doi S et al. Mesenchymal stem cells ameliorate experimental peritoneal fibrosis by suppressing inflammation and inhibiting TGF-beta1 signaling. *Kidney Int* 2013;84:297–307.

29 Huang W, Wang T, Zhang D et al. Mesenchymal stem cells overexpressing CXCR4 attenuate remodeling of postmyocardial infarction by releasing matrix metalloproteinase-9. *Stem Cells Dev* 2012;21:778–789.

30 Salamon A, Adam S, Rychly J et al. Long-term tumor necrosis factor treatment induces NFkappaB activation and proliferation, but not osteoblastic differentiation of adipose tissue-derived mesenchymal stem cells in vitro. *Int J Biochem Cell Biol* 2014;54:149–162.

31 Olobo JO, Geletu M, Demissie A et al. Circulating TNF-alpha, TGF-beta, and IL-10 in tuberculosis patients and healthy contacts. *Scand J Immunol* 2001;53:85–91.

32 Thompson CD, Zurko JC, Hanna BF et al. The therapeutic role of interleukin-10 after spinal cord injury. *J Neurotrauma* 2013;30: 1311–1324.

33 Zheng WD, Zhang LJ, Shi MN et al. Expression of matrix metalloproteinase-2 and tissue inhibitor of metalloproteinase-1 in hepatic stellate cells during rat hepatic fibrosis and its intervention by IL-10. *World J Gastroenterol* 2005;11:1753–1758.

34 Kim JS, Kim JG, Moon MY et al. Transforming growth factor-beta1 regulates macrophage migration via RhoA. *Blood* 2006;108: 1821–1829.

35 Narine K, De Wever O, Van Valckenborgh D et al. Growth factor modulation of fibroblast proliferation, differentiation, and invasion: Implications for tissue valve engineering. *Tissue Eng* 2006;12:2707–2716.

36 Kim JS, Cha SH, Kim WS et al. A novel therapeutic approach using mesenchymal stem cells to protect against *Mycobacterium abscessus*. *STEM CELLS* 2016;34:1957–1970.



See [www.StemCellsTM.com](http://www.StemCellsTM.com) for supporting information available online.